

Climate and Ocean Dynamics and the Lead Isotopic Records in Pacific Ferromanganese Crusts

John N. Christensen, Alex N. Halliday, Linda V. Godfrey,
James R. Hein, David K. Rea

As hydrogenous iron-manganese crusts grow, at rates of millimeters per million years, they record changes in the lead isotopic composition of ambient seawater. Time-resolved lead isotopic data for cut slabs of two central Pacific iron-manganese crusts that have been growing since about 50 million years ago were measured *in situ* by laser ablation, multiple-collector, inductively coupled plasma mass spectrometry. The lead isotopic compositions have remained remarkably uniform over the past 30 million years, but the record of small variations corresponds with other paleoceanographic indicators of climate change, including weathering and glaciation. This implies that despite the short residence time of lead in the oceans, global mechanisms may influence lead isotopic compositions in the central Pacific, far from continental inputs, because of changes in weathering, ocean circulation, and degree of mixing. Thus lead isotopic data could be used to probe climate-driven changes in ocean circulation through time.

The dynamics of Earth's atmosphere-ocean system are controlled in part by the poleward energy transfer mediated by major ocean currents. Furthermore, changes in continental weathering and riverine contributions to the oceans may also be linked with climate, and hydrothermal inputs vary with tectonism. A record of these past changes should be retrievable from the variations in isotopic compositions of elements in pristine seawater precipitates (chemical sediments) such as carbonates and hydrogenous Fe-Mn crusts (1–7). However, interpretations of these records have often been controversial. Until recently, little use has been made of records of Pb isotopic variations in the oceans, because the recent record is strongly affected by anthropogenic contributions and because a well-preserved record has been difficult to acquire. Lead and Nd isotopic records from Fe-Mn crusts have been obtained by thermal ionization mass spectrometry (4, 6). The new technique of laser ablation, multiple-collector, inductively coupled plasma mass spectrometry (LA-MC-ICPMS) has the advantage over conventional Pb isotopic techniques in that rapid and reproducible high-precision Pb isotopic data can be acquired directly from a cut slab of Fe-Mn crust (8). Using this technique, we show here that the Pb in central Pacific Ocean deep water, well away

from the continents, fluctuated in its isotopic composition over the past 50 million years and that these fluctuations are similar to records of major paleoceanographic and paleoclimatic changes.

Ferromanganese crusts. The Fe-Mn crusts we studied were dredged from central Pacific seamounts. Both of these crusts have been analyzed for Sr, Nd, Pb, and Be isotopic compositions (4, 6, 9). Crust CD29-2 (16°42.4'N, 168°14.2'W) was recovered from a depth of 2.3 km from Karin Ridge in the Johnston Island Economic Exclusion Zone (Line Islands) south of the Hawaiian Ridge (Fig. 1). It is ~10 cm thick, well preserved, and formed on a substrate of altered hyaloclastite that is partly phosphatized and cut by carbonate fluorapatite (CFA) veins. Crust D11-1 (11°39'N, 161°41'E) is from the Marshall Islands at a locality 3250 km to the west of that of CD29-2. D11-1 was recovered from a depth of 1.8 km, is ~15 cm thick, and was deposited on an altered hyaloclastite substrate. Layers in CD29-2 contain from 89 to 96 volume % δ -MnO₂ (vernadite); 1 to 4% quartz plus plagioclase; and, below 50 mm from the crust surface, 7 to 10% CFA. Layers in D11-1 vary from 71 to 100% δ -MnO₂; 1 to 3% quartz plus plagioclase; and, below 40 mm from the crust surface, 14 to 29% CFA (10). In both crusts, iron content varies between 9 and 15 weight %, Mn varies from 18 to 20 weight %, and Pb varies from 670 to 1500 parts per million (ppm). Growth rates of Fe-Mn crusts can be measured with the use of ¹⁰Be/⁹Be data, and reliable ages extend back to approximately 10 million years ago (Ma). Measured growth rates (4) are 2.1 mm per million years (My) for crust CD29-2 (since 10 Ma) and 1.4 mm/My (since 6 Ma) and 2.7 mm/My (from 7 to 10 Ma) for D11-1. Linear extrapolation of these growth rates would indicate that the crusts started growing about 55 to 60 Ma (4, 11). At that time, CD29-2 and D11-1 were in a larger ocean than now and were located close to the equator, on the basis of reconstructed Pacific plate motions (12).

Lead isotope stratigraphy. The results of LA-MC-ICPMS isotopic analyses (13) (Fig. 2) agree very well with conventional Pb isotopic data for corresponding positions, as demonstrated for CD29-2, and can be converted into well-defined changes in composition with time (Fig. 3) with the use of the respective growth rates (4). With a growth rate of 2.1 mm/My for crust CD29-2, each analysis raster represents the Pb isotopic

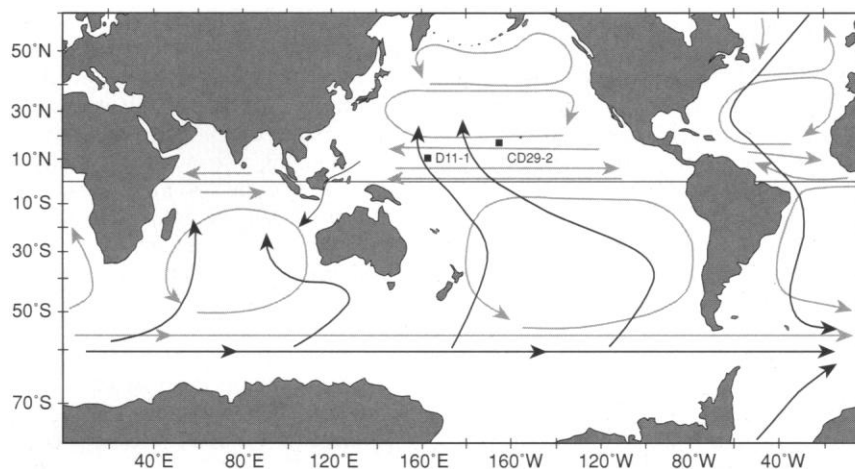


Fig. 1. Map of the Pacific Ocean showing the sample locations of the two Fe-Mn crusts. Schematic representations of surface currents are shown as grey arrows, and deep water flow is shown as black arrows (38).

J. N. Christensen, A. N. Halliday, and D. K. Rea are at the Department of Geological Sciences, University of Michigan, 2534 C. C. Little Building, Ann Arbor, MI 48109, USA. L. V. Godfrey is at the Department of Geological Sciences, Cornell University, Ithaca, NY 14853, USA. J. R. Hein is with the U.S. Geological Survey, 345 Middlefield Road, MS999, Menlo Park, CA 94025, USA.

composition of seawater averaged over ~75,000 years. The overall pattern for the two crusts is that they started growing with distinct Pb isotopic compositions that varied in tandem and converged through the Cenozoic. From a depth in crust CD29-2 (from the Line Islands) of 103 mm (49 Ma), $^{207}\text{Pb}/^{206}\text{Pb}$ and $^{208}\text{Pb}/^{206}\text{Pb}$ ratios rise to a local maximum at 62 mm (30 Ma) (Figs. 2 and 3). Between 62 and 33 mm from the surface (30 to 16 Ma), the ratios are variable but gradually decrease to a minimum at ~16 Ma and then rise to another maximum at 24 mm (about 10 Ma), followed by a minimum at 8 mm (4 to 5 Ma). The ratios rise again between 8 and 4 mm (4 to 2 Ma). Within the last 4 mm (<1.7 Ma), the ratios are lower than the maximum at 10 Ma.

The record for crust D11-1 from the Marshall Islands is similar to that of CD29-2 between 2 and 10 Ma (Figs. 2 and 3) (the surface layers were not sampled), but as a whole the crust displays less isotopic variability. The records differ before 10 Ma, especially before 30 Ma, but the crusts exhibit similar Pb isotopic changes from the earliest part of the record. For example, both crusts display an increase in $^{208}\text{Pb}/^{206}\text{Pb}$ ratios until ~45 Ma, producing a peak at ~43 Ma even though the absolute values are offset and the shapes of the curves differ. From 30 to 15 Ma, the pattern of D11-1 roughly tracks and parallels that of CD29-2 but at higher $^{208}\text{Pb}/^{206}\text{Pb}$ and $^{207}\text{Pb}/^{206}\text{Pb}$ ratios. Minima occur in both crusts at 22, 16, and 5 Ma, with intervening peaks at 18 and 10 Ma. However, a difference in the timing of early $^{206}\text{Pb}/^{204}\text{Pb}$ ratio changes is found (Fig. 3). In CD29-2, the $^{206}\text{Pb}/^{204}\text{Pb}$ ratio drops from 18.9 before 45 Ma to 18.6 by 30 Ma, whereas in D11-1, the major drop in $^{206}\text{Pb}/^{204}\text{Pb}$ ratio appears to occur earlier, between 55 and 50 Ma.

That the records show sympathetic offsets and, ultimately, identical values, is evidence that the entire record in each crust is well preserved. The lower parts of each crust (pre-20 Ma in D11-1 and pre-26 Ma in CD29-2) are phosphatized (4), but there is no indication that this alteration affects the Pb isotopic variations, even though some Pb was likely transferred to the CFA phase (14). The $^{208}\text{Pb}/^{206}\text{Pb}$ ratios change in parallel in the two crusts, between ~33 and ~15 Ma, through the phosphatization boundaries in each crust (Fig. 3). Any transfer of Pb within the crust because of phosphatization or other diagenetic processes should have homogenized isotopic gradients, whereas the Pb isotopic variations in both crusts are clear and sympathetic, even in the earliest history of the crusts (Fig. 3). The extrapolation of the growth rates from 10 Ma back to the early Cenozoic is uncertain, but the observation

that the crusts have coeval increases and decreases in isotopic composition, despite differing extrapolated growth rates, implies that the extrapolations are essentially correct. Caution should nonetheless still be exercised in interpreting the apparent difference in the early timing of the $^{206}\text{Pb}/^{204}\text{Pb}$ ratio changes (Fig. 3).

Correlation with global change. A rough correspondence is found between temporal changes in Pb isotopic compositions of the Fe-Mn crusts and the oxygen isotopic composition ($\delta^{18}\text{O}$) of benthic foraminifera (15) (Fig. 3). The large shift in $\delta^{18}\text{O}$ between 33 and 30 Ma (just after the Eocene/Oligocene boundary) corresponds to a significant rise in $^{207}\text{Pb}/^{206}\text{Pb}$ and $^{208}\text{Pb}/^{206}\text{Pb}$ ratios in CD29-2. In D11-1 the corresponding excursion is smaller but still discernible, and the $^{208}\text{Pb}/^{206}\text{Pb}$ ratio reaches a culmination at ~30 Ma. Between 30 and 16 Ma, $\delta^{18}\text{O}$ and the $^{208}\text{Pb}/^{206}\text{Pb}$ ratio of both crusts decrease in unison, reaching a new minimum that is followed by a rapid increase in these parameters after 16 Ma. The rapid rise in $\delta^{18}\text{O}$ at about 5 Ma is associated with reversals in trends of $^{208}\text{Pb}/^{206}\text{Pb}$ and $^{207}\text{Pb}/^{206}\text{Pb}$ ratios in both crusts. The correlation between these variables is revealed more clearly by plots of the residuals from the best-fit lines through the data for each crust and for each $\delta^{18}\text{O}$ record (Fig. 3). This subtracts the long-term (50-My) trends from the records, allowing a more direct comparison of the shorter term variations in the records. It can be seen that $^{208}\text{Pb}/^{206}\text{Pb}$ ratio and $\delta^{18}\text{O}$ track each other well. The changes in Pb isotopic composition thus seem somehow to relate to ocean temperature and continental ice volume (as reflected in the benthic foraminifera $\delta^{18}\text{O}$ record) and hence to climate.

These data present something of a paradox. Isotopic variations in Pb are expected to reflect changes in localized inputs because of its supposedly short residence time and wide variation in source composition of rocks (9, 16, 17). However, the data indicate that global forcing mechanisms appear to be controlling the isotopic composition of Pb reaching the central Pacific. The convergence of the two Pb isotopic records through time may be a function of gradual changes in ocean circulation or an increased efficiency of mixing, or both. However, the synchronicity of the deviations since ~30 Ma (Fig. 3) implies additional mechanisms that produce global changes in Pb and O isotopic composition on short time scales.

As with better-established isotopic proxies such as Sr (1), the critical parameters that affect changes in Pb might be expected to include the relative contributions of erosion of the continents versus seafloor hy-

drothermal activity. However, unlike Sr, the residence time of Pb in central Pacific deep water is short (currently 80 to 400 years) relative to the mixing time of the oceans (16). Because of its short residence time, the isotopic composition of Pb in paleoseawater is variable within and among ocean basins (9, 16, 17). Therefore, local changes are expected to affect the Pb isotopic records of widely separated Fe-Mn crusts. Eolian fluxes, local hydrothermal activity, specific riverine sources, and the intensity and direction of ocean currents advecting water from different ocean basins could all be important. Despite this, the

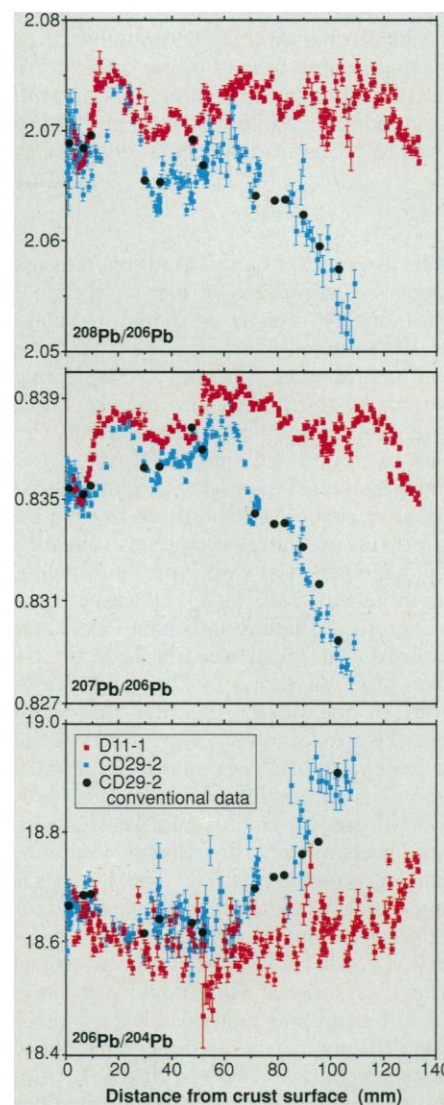


Fig. 2. Plots of distance from the surface of crusts for CD29-2 (blue boxes) and D11-1 (red boxes) versus $^{208}\text{Pb}/^{206}\text{Pb}$ (top), $^{207}\text{Pb}/^{206}\text{Pb}$ (middle), and $^{206}\text{Pb}/^{204}\text{Pb}$ (bottom) ratios. Conventional analyses of CD29-2 are shown as solid black circles. Uncertainties are all shown at the 2σ level. CD29-2 is phosphatized below 50 mm depth, whereas D11-1 is phosphatized below 40 mm depth (4, 9).

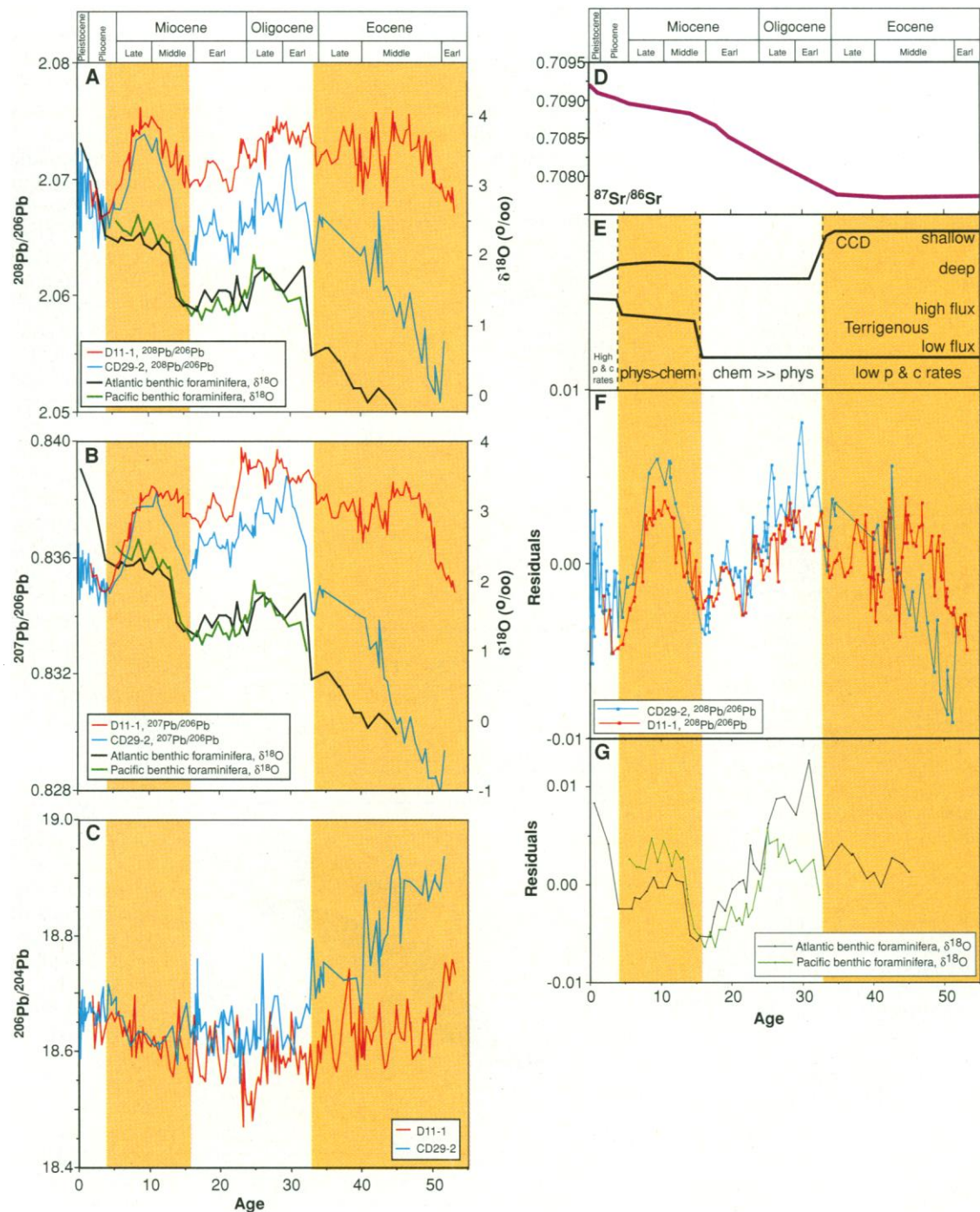
total variation in Pb isotopic composition is small [see also (4, 9)] compared with the gross heterogeneity in nonanthropogenic contributions provided by the world's riverine (19), eolian (20), and hydrothermal (21) fluxes (Fig. 4A). Given the major erosional, plate tectonic, volcanic, and climate changes in and around the Pacific basin, it is striking that the Pb isotopic composition of central Pacific seawater seems to have varied so little over almost the entire Cenozoic. Similarly, even the most extreme coeval differences between the two crusts

during the early Cenozoic are small and are consistent with their relatively close proximity (~3000 km).

Lead sources. Identification of specific sources for the Pb is difficult. Data for distinct parts of the crusts define different but subparallel linear Pb isotopic arrays that are most strikingly displayed in CD29-2 (Fig. 4C). These arrays are replicated by conventional Pb isotopic data for corresponding positions in the crust. For CD29-2, the lower array (A) represents data from the periods 0 to 6 Ma and 32 to 39 Ma, which

were times of growth of the two major continental ice sheets, whereas the upper array (B) represents data from 7 to 31 Ma. Data from 7 to 16 Ma may form a third array with a slightly lower slope than the data for 17 to 31 Ma, whereas data from 40 to 50 Ma forms an offset array (C) with a connecting portion to array A. Thus, one or both of the mixing end-members changed at least three times during the growth of this crust. The D11-1 crust shows much less variation in $^{207}\text{Pb}/^{206}\text{Pb}$ and $^{208}\text{Pb}/^{206}\text{Pb}$ ratios. Data for the past ~6 Ma and ~50 to

Fig. 3. The Pb isotopic records of CD29-2 and D11-1 compared with (A and B) the $\delta^{18}\text{O}$ of benthic foraminifera (15). (C) Age versus $^{206}\text{Pb}/^{204}\text{Pb}$ ratio for CD29-2 and D11-1. (D) Age versus seawater $^{87}\text{Sr}/^{86}\text{Sr}$ ratio (1, 39). (E) The changes in CCD (26) and terrigenous fluxes to the oceans (27). (F) Residuals for the Pb isotopic records of CD29-2 and D11-1 compared with (G) residuals for the Pacific and Atlantic records of $\delta^{18}\text{O}$ of benthic foraminifera (15). The residuals for the Atlantic and Pacific $\delta^{18}\text{O}$ were calculated separately. Yellow shading highlights major changes in the Pb isotopic records as well as periods of different climatic and erosional conditions in the Cenozoic. Along the bottom of each panel, the distance scale for each crust has been converted into time with the use of the $^{10}\text{Be}/^9\text{Be}$ data of Ling *et al.* (4).



55 Ma coincide with array A of CD29-2, whereas data for 11 to 49 Ma form arrays overlapping the upper portion of array B of CD29-2 (Fig. 4C).

There is no proximal source of Pb that would be expected to produce such Pb isotopic compositions or variations with time. The most local potential sources are submarine hydrothermal activity and eolian dust. The record of Hawaiian volcanism is reasonably well established for the time since 40 Ma and clearly does not match the Pb isotopic variations in CD29-2. Furthermore, hot-spot volcanism is unlikely to be linked with climate. Hydrothermal Pb derived from Pacific mid-ocean ridge basalt (MORB) is known to be transported considerable distances (~1000 km) in particles carried by hydrothermal plumes (22), and the degree to which such Pb is dissolved and transported within general ocean circulation is unclear (9, 23). The Pb isotopic

data from the Fe-Mn crusts converge near the average Pb isotopic composition of Pacific and Atlantic MORBs (Fig. 4B). MORBs from the Pacific and Indian oceans have distinct Pb isotopic compositions; therefore, hydrothermal Pb from such sources should also be distinct. Recent Pb isotopic data for Indian (9, 18) and Pacific (9) Fe-Mn crusts trend toward their respective MORB compositions (Fig. 4B), which indicates that MORB-derived Pb may be contributing a dissolved component to seawater. Whether this is of hydrothermal origin or is recycled in some manner, such as by oxidation of sulfides or through subduction zone volcanism and subsequent erosion of arcs (9), is unclear. The data do not align perfectly with the Pacific MORB average in all Pb isotopic ratio plots, but the possibility remains that hydrothermal Pb provides some of the coeval transient isotopic excursions in the crusts. Such a source is not

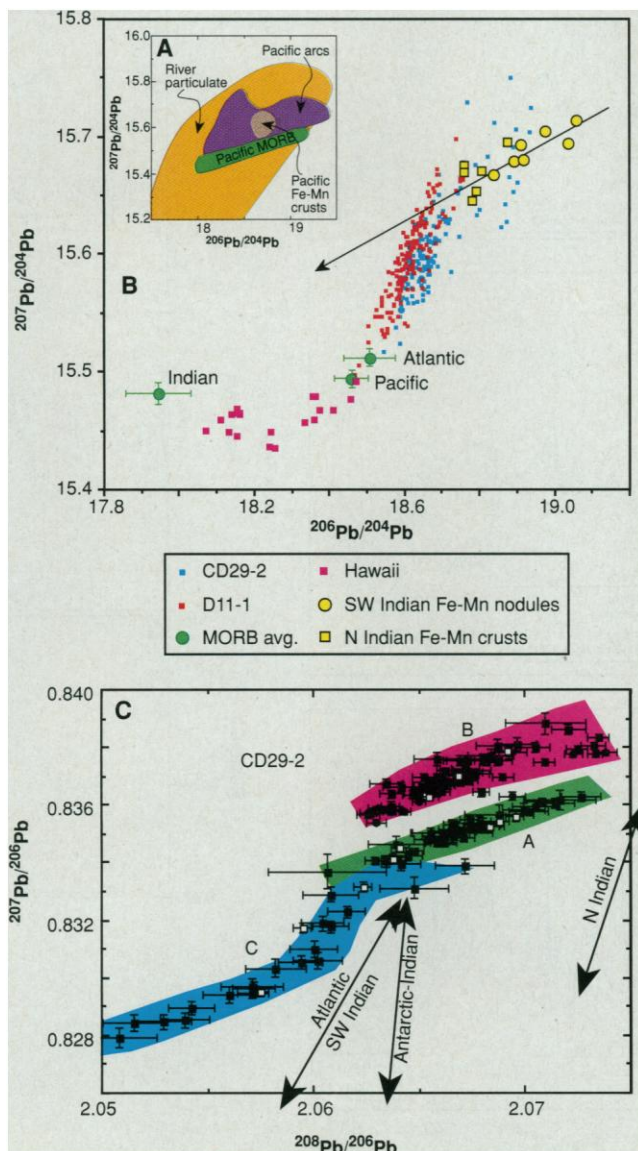
expected to yield the overall correspondence with O isotopic excursions. Therefore we infer that a major component of the Pb must be of continental origin if there is a link with climate.

Eolian inputs of recent nonanthropogenic Pb are isotopically well characterized for the Pacific Ocean and, as with Nd, show no geographical relation to variations in Fe-Mn crust Pb isotopic composition (20). The flux of dust reaching the North Pacific has increased dramatically by more than an order of magnitude since ~3 Ma (24) but in general does not correspond with the Pb isotopic records of the crusts. There has been no systematic variation in Pb isotopic composition in dust to the North Pacific since 12 Ma (25). Therefore, variations in the nature or flux of eroded dust are an unlikely cause of the Pb isotopic variations in the crust.

Erosion and lead isotopes. Changes in climate and tectonism and the type of exposed continental crust might be expected to produce changes in Pb isotopic composition. The long-term changes in calcite compensation depth (CCD) (26) and seawater $^{87}\text{Sr}/^{86}\text{Sr}$ ratios (1) appear to be dominated by the effects of continental weathering (27). These and other data imply that both physical weathering and chemical weathering were slow through the Paleocene and Eocene (27) (Fig. 3). Both the CCD and seawater $^{87}\text{Sr}/^{86}\text{Sr}$ ratios indicate that weathering has increased since the Eocene/Oligocene boundary (33 to 34 Ma). Both the Pb data in the crusts and the $\delta^{18}\text{O}$ values change at the Eocene/Oligocene boundary (Fig. 3). Furthermore, the residuals of the two Pb curves track each other closely after this time (Fig. 3). Chemical weathering was high from 33 to 15 Ma, as evidenced by a deep CCD, and during this time Pb and O isotopes changed gradually (Fig. 3). In the mid- to late-Miocene (~15 to 10 Ma), mechanical weathering intensified, as recorded in the terrigenous flux to the oceans (27, 28) (Fig. 3). Again, the CCD and Pb and O isotopic records seem to reflect such changes (Fig. 3). Since about 5 Ma, the relation among the depth of the CCD and the amounts of Pb and O isotope composition has become more obscure (Figs. 3 and 4) as physical and chemical weathering rates have peaked.

The isotopic compositions of Sr, Pb, and Os leached from soils have been shown to change as weathering becomes more intense (29–31). Some have attributed the changes in Sr (29) and Os (30) isotopic composition in seawater to such disequilibrium effects. It has been shown that $^{207}\text{Pb}/^{206}\text{Pb}$ ratios increase with degree of weathering in soils from Sierra Nevada granitoids

Fig. 4. (A) A plot of $^{206}\text{Pb}/^{204}\text{Pb}$ versus $^{207}\text{Pb}/^{204}\text{Pb}$ ratios, showing fields for Pacific MORB, river particulates (19), Pacific arcs, and data for recent layers of Pacific Fe-Mn crusts (9). (B) Plot of $^{206}\text{Pb}/^{204}\text{Pb}$ versus $^{207}\text{Pb}/^{204}\text{Pb}$ ratios, displaying data for CD29-2 (blue), D11-1 (small red squares), and crusts and nodules from the Indian Ocean (9, 18) (yellow) together with average Pacific, Atlantic, and Indian Ocean MORBs (green) (40). The CD29-2 and D11-1 data trend toward the averages of Pacific and Atlantic MORBs, whereas the Indian Ocean samples form an array in line with average Indian MORB. (C) A plot of $^{208}\text{Pb}/^{206}\text{Pb}$ versus $^{207}\text{Pb}/^{206}\text{Pb}$ ratios, displaying data for CD29-2. Conventional analyses of CD29-2 are shown as white squares; laser analyses are shown as black squares. All errors are shown at the 2σ level. The data defining array A are for the periods from 0 to 6 Ma and 32 to 39 Ma; data defining array B are for 17 to 31 Ma; and data defining array C represent 50 to 40 Ma. Arrows represent mixing trajectories defined by data for recent samples of circum-Antarctic nodules and Atlantic and Indian crusts (9, 18).



(31). Such disequilibrium effects are not recognizable in the Fe-Mn crust data. Increasing degrees of chemical weathering during the Oligocene and early Miocene are accompanied by decreasing $^{207}\text{Pb}/^{206}\text{Pb}$ and $^{208}\text{Pb}/^{206}\text{Pb}$ ratios, an effect that is the opposite of that predicted by this model. The major changes in Pb isotopic ratios occurred during the Eocene, when global weathering rates are thought to have been at their lowest. Therefore, although the Pb isotopic compositions appear to be responding to changes in weathering, the mechanisms are not well understood.

Ocean circulation and lead isotopes. The $\delta^{18}\text{O}$ data provide an indication of ocean temperature and continental ice volume rather than weathering flux per se. One reason that the Pb isotope data might covary with O isotopes is that the isotopic composition of Pb in the central Pacific should be a sensitive indicator of changes in the mixture of Pb being incorporated into oceanic circulation on regional or perhaps global scales. The central Pacific deep water sampled by the Fe-Mn crusts is now approximately 1600 years old and has migrated from the Atlantic through the Indian Ocean and northward from the southern Pacific (32) (Fig. 1). Changes in temperature gradients between surface and deep water and latitudinal gradients should result in changes in the efficiency of mixing, and the Pb isotopic data are sensitive to this because the residence time is shorter than the mixing time of the oceans.

The similarity of the Pb isotopic records for the two crusts after 30 Ma implies a change in regime from relatively poor mixing in the Eocene, which is consistent with warmer temperatures and reduced latitudinal temperature gradients during that period (33), to extensive mixing after 30 Ma. The approximately constant difference between the two records from 30 to 10 Ma indicates that homogenization and mixing of the Pb isotopic signal reaching the sample localities was not as effective on a 10^3 -km length scale as it has been since ~ 10 Ma. This effect is consistent with the distributions of foraminifera, which indicate that east-west equatorial provinciality has decreased in the Pacific Ocean since 10 Ma, which is attributed to strengthening of Pacific surface water circulation and the establishment of the Pacific equatorial undercurrent in response to the restriction of the Indonesian Seaway (34).

The radiogenic Pb in the Eocene portions of the crusts (lower $^{207}\text{Pb}/^{206}\text{Pb}$ and higher $^{206}\text{Pb}/^{204}\text{Pb}$ ratios) is similar to that in the most recent layers of crusts and nodules from the Indian, Atlantic, and circum-Antarctic oceans. This may reflect changes

in ocean gateways. During the Cenozoic, Australia moved northward away from Antarctica (35), restricting the gap between Indonesia and Australia (36) and allowing exchange between the Indian and Pacific Oceans through the Antarctic Ocean. Over this same time interval, Tethys closed, and equatorial surface waters were exchanged between the Pacific and the Atlantic through the gap between North and South America before formation of the Panama Isthmus by ~ 3 Ma (37). CD29-2 is from a region of relatively old ocean floor, and it would have sampled deep water throughout its history, whereas D11-1 may have sampled surface waters before 30 Ma. Therefore, the differing records may reflect a combination of changes in circulation and differences in the subsidence histories of the two sample locations. Analysis of Fe-Mn crusts from other oceans should clarify the relative importance of such gateways in Pb isotopic changes. The isotopic composition of Pb in the central Pacific has in fact varied remarkably little over the past 30 Ma [see also (4)] and has been essentially homogeneous over 3000 km for most of that period. Despite this, the clearly resolvable small changes in the Pb isotopic compositions of central Pacific seawater appear to provide an interesting new proxy for changes in climate, weathering, and the vigor of ocean circulation.

REFERENCES AND NOTES

- J. Hess, M. L. Bender, J.-G. Schilling, *Science* **231**, 979 (1986).
- B. Peucker-Ehrenbrink, G. Ravizza, A. W. Hofmann, *Earth Planet. Sci. Lett.* **130**, 155 (1995).
- J. R. Hein, W. A. Bohron, M. S. Schulz, *Paleoceanography* **7**, 63 (1992).
- H. Ling *et al.*, *J. Conf. Abstr.* **1**, 361 (1996); H. Ling *et al.*, *Earth Planet. Sci. Lett.* **146**, 1 (1996).
- F. Chabaux, A. S. Cohen, R. K. O'Nions, J. R. Hein, *Geochim. Cosmochim. Acta* **59**, 633 (1995).
- F. von Blanckenburg, R. K. O'Nions, N. S. Belshaw, A. Gibb, J. R. Hein, *Earth Planet. Sci. Lett.* **141**, 213 (1996).
- K. W. Burton, H. F. Ling, R. K. O'Nions, *Nature* **386**, 382 (1997).
- A. J. Walder, I. D. Abell, A. I. Platzner, P. A. Freedman, *Spectrochim. Acta* **48**, 397 (1993); J. N. Christensen, A. N. Halliday, D.-C. Lee, C. M. Hall, *Earth Planet. Sci. Lett.* **136**, 79 (1995); A. N. Halliday *et al.*, *Int. J. Mass Spectrom. Ion Process.* **146/147**, 21 (1995); A. N. Halliday *et al.*, *Soc. Econ. Geol. Short Course*, in press.
- F. von Blanckenburg, R. K. O'Nions, J. R. Hein, *Geochim. Cosmochim. Acta* **60**, 4957 (1996).
- J. R. Hein *et al.*, *U.S. Geol. Surv. Open-File Rep.* **90-407** (1990).
- The Pb isotopic records were calibrated in time by linear extrapolation of the respective $^{10}\text{Be}/^9\text{Be}$ growth rates (4) from the surfaces of each crust.
- D. Engebretson, A. Cox, R. Gordon, *Geol. Soc. Am. Spec. Pap.* **206** (1985).
- The Pb isotopic analyses were conducted with the use of an ultraviolet (UV) laser to ablate the samples. The UV laser beam was moved by computer control to raster areas $100\ \mu\text{m}$ by $150\ \mu\text{m}$. For each analysis, data were collected for ~ 5 min, during which time approximately $10\ \mu\text{g}$ of material was ablated from the crust, producing a crater $400\ \mu\text{m}$ deep. The ablated material was immediately carried by a flow of Ar gas to the Ar plasma source of an MC-ICPMS. Masses 202 through 208 were measured simultaneously with the use of a set of adjustable Faraday collectors. The $^{203}\text{Tl}/^{205}\text{Tl}$ of Tl that occurs naturally in the Fe-Mn crust was monitored during analysis and used to correct for mass fractionation of the Pb isotopic ratios (8). Mass interference of ^{204}Hg on ^{204}Pb was corrected for by monitoring ^{202}Hg and was typically 1% or less. One hundred thirty-four analyses of CD29-2 were conducted along a traverse from the surface of the crust toward the substrate with a VG MicroProbe UV laser. In the case of D11-1, 163 analyses were conducted with a Cetac LSX-100 UV laser. For comparison, a set of 13 samples of CD29-2 were taken by mechanical means along a parallel traverse and analyzed by conventional chemical and mass spectrometric methods. Conventional Pb isotopic analyses were conducted at Cornell and were corrected for mass discrimination with the use of the measured values of NIST SRM 981, which were as follows: $^{206}\text{Pb}/^{204}\text{Pb} = 16.937$, $^{207}\text{Pb}/^{204}\text{Pb} = 15.493$, and $^{208}\text{Pb}/^{204}\text{Pb} = 36.705$. The averages in run precisions with LA-MC-ICPMS were $\pm 0.09\%$ for $^{206}\text{Pb}/^{204}\text{Pb}$, $^{207}\text{Pb}/^{204}\text{Pb}$, and $^{208}\text{Pb}/^{204}\text{Pb}$; $\pm 0.02\%$ for $^{207}\text{Pb}/^{206}\text{Pb}$; and $\pm 0.03\%$ for $^{208}\text{Pb}/^{206}\text{Pb}$; which compare well with conventional analyses. At the time of these analyses, LA analyses of SRM 611 yielded $^{207}\text{Pb}/^{206}\text{Pb} = 0.90934 \pm 0.00033\ 2\sigma$ and $^{208}\text{Pb}/^{206}\text{Pb} = 2.1666 \pm 0.0016\ 2\sigma$. During the course of the traverse, we returned to stratigraphic positions at which major peaks in Pb isotopic composition were found to occur and verified their existence by replicate analysis. We also returned to stratigraphic positions intermediate to previously analyzed positions and produced data consistent with the adjacent analyses. Although the analyses will include any nonhydrogenous material present (such as eolian detritus), they still represent the Pb isotopic compositions of ambient seawater during growth of the crust because (i) the mass fraction of Pb in Fe-Mn oxide (~ 1000 ppm Pb) is 500 to 5000 times greater than in a possible eolian dust or detrital component (10 to 1% at 20 ppm Pb); (ii) the Pb is mainly hosted by Fe-Mn oxides, which are direct precipitates from seawater [Y.-H. Li, *Geochim. Cosmochim. Acta* **55**, 3223 (1991)]; and (iii) there is no correspondence between the high $^{206}\text{Pb}/^{204}\text{Pb}$ ratios of central Pacific eolian dust (20) and the much less radiogenic Pb of central Pacific Fe-Mn crusts (9). Therefore, it is likely that the observed patterns in Pb isotopic composition faithfully record the isotopic composition of ambient seawater from which the crust grew.
- A. Koschinsky and P. Halbach, *Geochim. Cosmochim. Acta* **59**, 5113 (1995).
- K. G. Miller, R. G. Fairbanks, G. S. Mountain, *Paleoceanography* **2**, 1 (1987). This time scale has been updated [W. A. Berggren *et al.*, *Soc. Econ. Paleontol. Mineral.* **54**, 129 (1995)].
- The residence time in seawater governs the scale of homogenization and limits the distance water masses may travel and still maintain a distinct Pb isotopic composition. The shorter the residence time, the more distinguishable local sources of Pb become. The mean residence time of an element in the open ocean can be estimated by calculating the ratio of the ocean reservoir for the element to either the total river flux that reaches the open ocean or the total flux to pelagic sediments [Y.-H. Li, *Geochim. Cosmochim. Acta* **46**, 2671 (1982)]. In the case of Pb, the natural Pb river flux is not well known because of anthropogenic additions. The Pb flux to pelagic sediments implies that the mean residence time is 10^2 years. But a similar calculation for Sm (which presumably has the same behavior as Nd) also implies a residence time of 10^2 years, rather than 10^3 years as indicated by river fluxes for Nd [C. J. Bertram and H. Elderfield, *Geochim. Cosmochim. Acta* **57**, 1957 (1993)]. Although this difference in behavior may be due to the greater scavenging of Pb by particulates, it is possible that the mean residence time of Pb has been underestimated. Studies of radioactive ^{210}Pb in seawater provides an alternative means of estimating the residence time of stable Pb isotopes. For

the north central Pacific, the estimated residence time of ^{210}Pb at mid-depths is 200 to 400 years, decreasing to 80 to 100 years toward the Pacific margins [Y. Nozaki, K. K. Turekian, K. von Damm, *Earth Planet. Sci. Lett.* **49**, 393 (1980); H. Craig, S. Krishnaswami, B. L. K. Somayajulu, *ibid.* **17**, 295 (1973)]. Given the observed differences in the Pb isotopic composition of Mn crusts and nodules from different ocean basins (18), the residence time must be less than the $\sim 10^3$ -year mixing time of the oceans [W. S. Broecker and T.-H. Peng, *Tracers in the Sea* (Eldigio Press, Columbia Univ., Palisades, NY, 1982)] but in the central Pacific may be sufficiently long to mix and integrate differing inputs from incoming water masses and the basin margins. Studies of ^{210}Pb indicate residence times in the upper ocean of ~ 10 years [R. M. Sherrell, E. A. Boyle, B. Hamelin, *J. Geophys. Res.* **97**, 11257 (1992)], which are much shorter than the residence time in deep water. The most important mechanism for Pb transport to the deep sea is scavenging by particulates, particularly organic particulates [A. R. Flegal and C. C. Patterson, *Earth Planet. Sci. Lett.* **64**, 19 (1983)], which may have varied considerably in the geologic past because of changes in biologic productivity.

17. T. J. Chow and C. C. Paterson, *Geochim. Cosmochim. Acta* **26**, 263 (1962).
18. W. Abouchami and S. L. Goldstein, *ibid.* **59**, 1809 (1995).
19. Y. Asmerom and S. B. Jacobsen, *Earth Planet. Sci. Lett.* **115**, 245 (1993).
20. C. E. Jones, A. N. Halliday, D. K. Rea, R. M. Owen, *Eos* **77**, 320 (1996).
21. M. Tatsumoto, *Earth Planet. Sci. Lett.* **38**, 63 (1978).
22. T. J. Barrett, P. N. Taylor, J. Lugowski, *Geochim. Cosmochim. Acta* **51**, 2241 (1987).
23. L. V. Godfrey, R. A. Mills, H. Elderfield, E. Gurvich, *Mar. Chem.* **46**, 237 (1994); L. V. Godfrey *et al.*, *Earth Planet. Sci. Lett.*, in press.
24. D. K. Rea, *Rev. Geophys.* **32**, 159 (1994).
25. T. Pettke, D. K. Rea, A. N. Halliday, in *Seventh Annual V. M. Goldschmidt Conference Abstracts*, LPI contribution 921, 163 (Lunar and Planetary Institute, Houston, TX, 1997).
26. T. H. van Andel, *Earth Planet. Sci. Lett.* **26**, 187 (1975).
27. D. K. Rea, *GSA Today* **3**, 207 (1993).
28. ———, *AGU Monogr.* **70**, 387 (1992).
29. J. D. Blum, Y. Erel, K. Brown, *Geochim. Cosmochim. Acta* **57**, 5019 (1994); J. D. Blum and Y. Erel, *Nature* **373**, 415 (1995).
30. B. Peucker-Ehrenbrink and J. D. Blum, *Eos* **77**, 324 (1996).
31. Y. Erel, Y. Harlavan, J. D. Blum, *Geochim. Cosmochim. Acta* **58**, 5299 (1994).
32. M. Andree *et al.*, *Clim. Dyn.* **1**, 53 (1986).
33. J. C. Zachos, L. D. Stott, K. C. Lohmann, *Paleoceanography* **9**, 353 (1994).
34. J. P. Kennet, G. Keller, M. S. Srinivasan, *GSA Memoir No.* 163, 197 (1985).
35. C. R. Scotese and J. Golonka, *PALEOMAP Paleogeographic Atlas* (PALEOMAP Progress Report 20, Department of Geology, Univ. of Texas at Arlington, 1992); D. B. Walsh and C. R. Scotese, Plate Tracker version 1.2 (Department of Geology, Univ. of Texas at Arlington, 1995).
36. F. Woodruff and S. Savin, *Paleoceanography* **4**, 87 (1989).
37. L. Keigwin, *Science* **217**, 350 (1982).
38. M. G. Gross, *Oceanography* (Prentice-Hall, Englewood Cliffs, NJ, ed. 6, 1993).
39. D. A. Hodell, J. A. Mueller, J. A. McKenzie, G. A. Mead, *Earth Planet. Sci. Lett.* **92**, 165 (1989); D. A. Hodell, G. A. Mead, J. A. Mueller, *Chem. Geol.* **80**, 291 (1990); D. A. Hodell, J. A. Mueller, J. R. Garrido, *Geology* **19**, 24 (1991); J. S. Oslick, K. G. Miller, M. D. Feigenson, J. D. Wright, *Paleoceanography* **9**, 427 (1994); K. G. Miller, M. D. Feigenson, D. V. Kent, R. K. Olsson, *ibid.* **3**, 223 (1988); K. G. Miller, M. D. Feigenson, J. D. Wright, B. M. Clement, *ibid.* **6**, 33 (1991).
40. W. M. White, A. W. Hofmann, H. Puchelt, *J. Geophys. Res.* **92**, 4881 (1987).
41. This research was supported by a grant from the

U.S. Department of Energy. We thank F. von Blanckenburg and R. K. O'Nions for sending us a preprint describing their Pb isotopic work; B. Wilkinson, W. Broecker, S. Epstein, S. Savin, and K. Burton for helpful discussions; M. Johnson and C. M. Hall for

technical help; Cetac Technologies for use of one of their laser systems; and F. von Blanckenburg and an anonymous reviewer for their comments.

16 December 1996; accepted 19 June 1997

Neighborhoods and Violent Crime: A Multilevel Study of Collective Efficacy

Robert J. Sampson, Stephen W. Raudenbush, Felton Earls

It is hypothesized that collective efficacy, defined as social cohesion among neighbors combined with their willingness to intervene on behalf of the common good, is linked to reduced violence. This hypothesis was tested on a 1995 survey of 8782 residents of 343 neighborhoods in Chicago, Illinois. Multilevel analyses showed that a measure of collective efficacy yields a high between-neighborhood reliability and is negatively associated with variations in violence, when individual-level characteristics, measurement error, and prior violence are controlled. Associations of concentrated disadvantage and residential instability with violence are largely mediated by collective efficacy.

For most of this century, social scientists have observed marked variations in rates of criminal violence across neighborhoods of U.S. cities. Violence has been associated with the low socioeconomic status (SES) and residential instability of neighborhoods. Although the geographical concentration of violence and its connection with neighborhood composition are well established, the question remains: why? What is it, for example, about the concentration of poverty that accounts for its association with rates of violence? What are the social processes that might explain or mediate this relation (1–3)? In this article, we report results from a study designed to address these questions about crime and communities.

Our basic premise is that social and organizational characteristics of neighborhoods explain variations in crime rates that are not solely attributable to the aggregated demographic characteristics of individuals. We propose that the differential ability of neighborhoods to realize the common values of residents and maintain effective social controls is a major source of neighborhood variation in violence (4, 5). Although social control is often a response to deviant behavior, it should not be equated with formal regulation or forced conformity by

institutions such as the police and courts. Rather, social control refers generally to the capacity of a group to regulate its members according to desired principles—to realize collective, as opposed to forced, goals (6). One central goal is the desire of community residents to live in safe and orderly environments that are free of predatory crime, especially interpersonal violence.

In contrast to formally or externally induced actions (for example, a police crackdown), we focus on the effectiveness of informal mechanisms by which residents themselves achieve public order. Examples of informal social control include the monitoring of spontaneous play groups among children, a willingness to intervene to prevent acts such as truancy and street-corner “hanging” by teenage peer groups, and the confrontation of persons who are exploiting or disturbing public space (5, 7). Even among adults, violence regularly arises in public disputes, in the context of illegal markets (for example, prostitution and drugs), and in the company of peers (8). The capacity of residents to control group-level processes and visible signs of social disorder is thus a key mechanism influencing opportunities for interpersonal crime in a neighborhood.

Informal social control also generalizes to broader issues of import to the well-being of neighborhoods. In particular, the differential ability of communities to extract resources and respond to cuts in public services (such as police patrols, fire stations, garbage collection, and housing code enforcement) looms large when we consider

R. J. Sampson is in the Department of Sociology, University of Chicago, Chicago, IL, 60637 and is a Research Fellow of the American Bar Foundation, Chicago, IL 60611, USA. S. W. Raudenbush is at the College of Education, Michigan State University, East Lansing, MI 48824, USA. F. Earls is the Principal Investigator of the Project on Human Development in Chicago Neighborhoods and is at the School of Public Health, Harvard University, Boston, MA 02115, USA.